Geologia Série Científica USP

Revista do Instituto de Geociências - USP

Geo. USP Sér. Cient., São Paulo, v.1, p. 1-15, novembro 2001

Petrography and Metamorphism of the Metasedimentary Country-Rocks of the Jacurici Valley Chromitite-Hosting Mafic-Ultramafic Complexes, Bahia, Northeastern Brazil.

Eliane A. Del Lama[1], Maria A. F. Candia[2], Gergely A. J. Szabó[2]

[1]FAPESP - pos-doctoral fellowship

[2]Departamento de Mineralogia e Geotectônica - Instituto de Geociências - USP

Rua do Lago 562, CEP 05508-900, São Paulo, SP

Keywords: Jacurici Valley, metasediments, metamorphism, metasomatism.

ABSTRACT

This paper deal with on the metasedimentary country-rocks of the chromite-bearing ultramafic rocks that occur in the "Jacurici River Valley Chromium District" northeastern Bahia, Brazil.

This region presents a complex geologic-petrologic framework of rocks that were intensely deformed, metamorphosed and transformed by metasomatic processes, making it difficult to interpret their evolutionary/metamorphic record.

Although the metasedimentary country rocks have also been affected by such processes, it is possible to distinguish evidence of a previous high-grade metamorphism that affected them.

Thermobarometric data for the observed mineralogical associations indicate P-T conditions around 750-800ºC and 7-8 kb for the metamorphic peak, based mainly on the presence of olivine in marbles and the cordierite-garnet-sillimanite-spinel association in aluminous gneisses.

Palavras-chave: Vale do Rio Jacurici, metassedimentos, metamorfismo, metassomatismo.

RESUMO

Este trabalho enfoca as encaixantes metassedimentares das rochas ultramáficas, portadoras de mineralização de cromita, que ocorrem no nordeste do estado da Bahia.

Esta região, conhecida como "Distrito Cromitífero do Vale do Rio Jacurici", apresenta grande complexidade geológica-petrológica com rochas intensamente deformadas, metamorfizadas e transformadas por processos metassomáticos, o que dificulta a interpretação do registro metamórfico/evolutivo dessas rochas.

Apesar dos metassedimentos também terem sido afetados pelos processos acima, é possível recuperar registros do metamorfismo de alto grau.

Dados termobarométricos indicam condições P-T de 750-800ºC e 7-8 kb, baseados na presença de olivina nos mármores e na associação cordierita-granada-sillimanita-hercinita nos gnaisses aluminosos.

INTRODUCTION

The study area is located in the Senhor do Bonfim ¼ degree sheet topographical map, Northeastern Bahia State, limited by the parallels 10º00' and 11º00'S and by the meridians 39º30' and 39º50'W (Figure 1), and belongs to the Jacurici River Valley Chromian District.

This work focuses on the country-rocks of the chromite-bearing ultramafic rocks that occur in the region. The country-rocks are represented by granulitic gneisses and other particular rock types such as marble, calc-silicate rocks, metaorthoclasite and aluminous gneiss. These particular rocks types will be detailed in this paper.

The area presents a complex geologic-petrologic framework with rocks intensely deformed, metamorphosed and transformed by metasomatic process, making it difficult to recover their evolutionary/metamorphic record.

Systematic geologic/petrologic investigations are scarce; only unpublished reports are available, made by request of the interested mining companies.

The aim of this paper is to describe the lithologic types not usually refered in published work, attempting to recover their original metamorphic imprint, as this kind of record is difficult to be recovered from the ultramafic rocks.

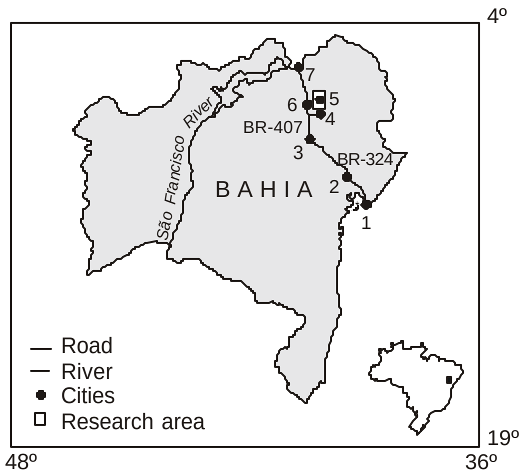

Figure 1: Localization and access roads of the researched area. (1- Salvador, 2- Feira de Santana, 3- Capim Grosso, 4- Itiúba, 5- Andorinha, 6- Senhor do Bonfim, 7- Juazeiro).

GEOLOGICAL SETTING

The chromite-bearing ultramafic rocks belong to the Caraíba Complex, outcropping along the Salvador-Curaçá Belt. The term Caraíba was used for the first time as a group by Barbosa (1964, 1970) for rocks that occur in the Curaçá river area. Figueiredo (1981) characterized this unit as a complex and studied its lithogeochemistry. Other denominations for this group are: Migmatitic-metamorphic Complex (CPRM, 1974 in Barbosa de Deus & Viana, 1982) and Pedra Vermelha Complex (Barbosa de Deus & Viana, 1982). The term Caraíba Complex is the designation adopted by Barbosa & Dominguez (1996) in the 1:1.000.000 Geological Map of Bahia State (Figure 2).

The Caraíba Complex is constituted predominantly by hypersthene-bearing gneisses with tonalitic to granitic composition. These rocks present grey-greenish colour when fresh, and brown when altered, and exhibit a penetrative foliation striking N-S with steep dips. Migmatitic structures are common, with gabbro-dioritic paleosome.

Barbosa & Dominguez (1996) interpret the Caraíba Complex rocks as belonging to the Transamazonic Cycle. In the Itabuna-Caraíba Complex, Silva *et al*. (1997) obtained U-Pb SHRIMP value of 2,695 Ma for the magmatic age and 2,072 Ma for the metamorphic age. Medrado mafic-ultramafic complex shows U-Pb in zircon age of 2,059 Ma (Oliveira, 1998).

Mafic-ultramafic bodies generally occur interlayered with layers and lenses of carbonatic/calc-silicate rocks, quartz and aluminous gneiss, iron formation and graphite-bearing schists. The sequence outcrops along a N-S direction parallel to the Itiúba Ridge located to the west (Figure 2), which is approximately 100 km long and 12 km wide. It has a syenitic composition and structural features indicating intrusive emplacement. The available Rb-Sr isotopic data point to an age around 2.0 Ga for this pluton (Conceição, 1990 in Barbosa & Dominguez, 1996).

The chromite-bearing bodies are generally thick, specially when compared with other chromitites of important stratiform complexes, including Campo Formoso. Although they usually exhibit thicknesses from 5 to 8 m they may attain thicknesses up to 15 m.

A possible stratigraphic sequence for the Jacurici Chromium District was proposed by Jardim de Sá (1984). From base to top he described:

-a Sequence of Supracrustal Rocks;

-Mafic-Ultramafic Bodies;

-G1 orthogneiss, with a predominantly acid composition, and displaying granulite facies parageneses. Several xenoliths of the supracrustal sequence are observed in this unit;

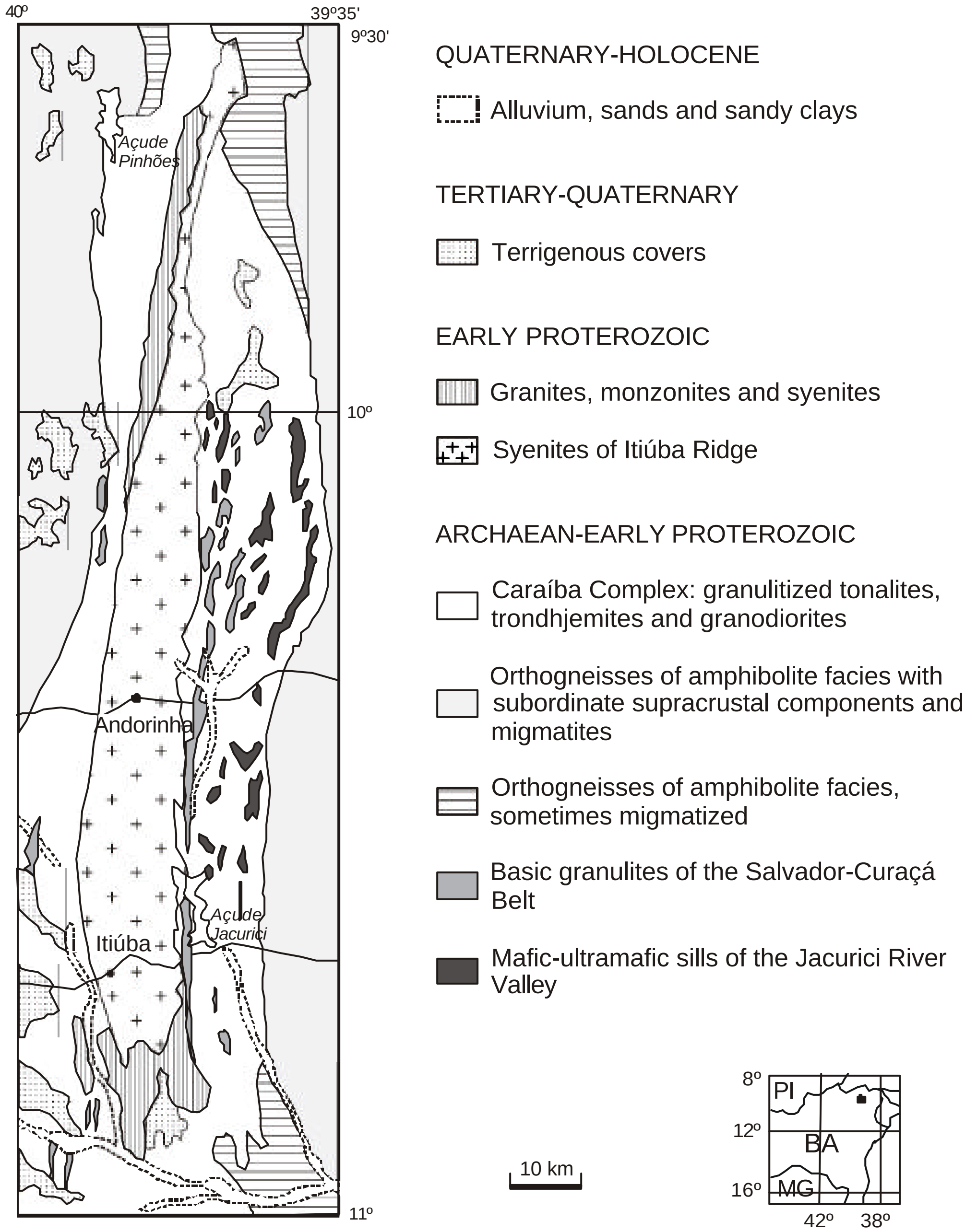

Figure 2: Geological map of the Jacurici River Valley area (Barbosa & Dominguez, 1996).

-Mafic Dykes, amphibolitized, with decimetric to metric thicknesses;

-G2 granodiorite and tonalite, orthogneiss, with thin metamorphic layering and granulite to amphibolite facies parageneses;

-G3 granites, represented by the Itiúba Syenite and equivalent dykes.

PETROGRAPHY

The metasedimentary rocks of the Jacurici River Valley Chromium District are represented by spinel-sillimanite-cordierite-garnet gneiss, metaorthoclasite, marble, diopsidite and metasomatic rocks (e.g., phlogopitite, phlogopite gneiss and garnet epidosite).

The marble and the diopsidite are more frequent. The other lithologies are of restricted occurrence, being generally found in drill holes.

Chemical analyses of representative minerals are listed in Tables 1-3. The samples were analysed by electron microprobe at the Instituto de Geociências - USP. Analyses were performed on the JXA-8600 Superprobe (JEOL) with an accelerating voltage of 15 kV and beam of 20 nA.

The mineral abbreviations are those of Kretz (1983).

Spinel-Sillimanite-Cordierite-Garnet Gneiss

This rock presents coarse granulometry with centimetric perthitic or mesoperthitic crystals. It is constituted by K-feldspar, quartz, cordierite, plagioclase, garnet, biotite, zircon and opaque minerals. Locally, sillimanite and green spinel also occur.

Plagioclase is albite (An_{6-10}) or oligoclase (An_{11-23}) – (Figure 3a).

Cordierite is distinguished by pinite alteration products. Locally less altered grains are preserved with sillimanite and/or spinel inclusions. It can also involve garnet grains. Its composition is Mg-rich (X_{Mg} = 0.8) – (Table 1).

Garnet is not very common. It shows poikiloblastic features and locally chloritized rims. Sillimanite and spinel inclusions occur, sillimanite being more common. It also appears as smaller crystals with subidioblastic to xenoblastic shapes. Garnet ($Alm_{57-68}Prp_{29-42}$) may be zoned or not. Zoned crystals have core compositions enriched in MgO and depleted in FeO relative to the rim (Figure 4).

Biotite and phlogopite exhibt brown pleochroism and occur as irregular and small crystals. They are Ti-rich (Figure 5b) with variable Fe and Mg contents (Figure 5d).

Opaques are associated with biotite and phlogopite. Zircon appears as small rounded crystals and generally develops weak pleochroic haloes in cordierite.

Spinel shows strong green tonality. Its composition is that of a gahnitic hercynite (X_{Fe} = 0.43-0.64). ZnO content varies from 6 to 11% and Fe content decreases with increasing Mg content. Spinels included in garnet are Mg-richer and Fe-poorer (Figure 6).

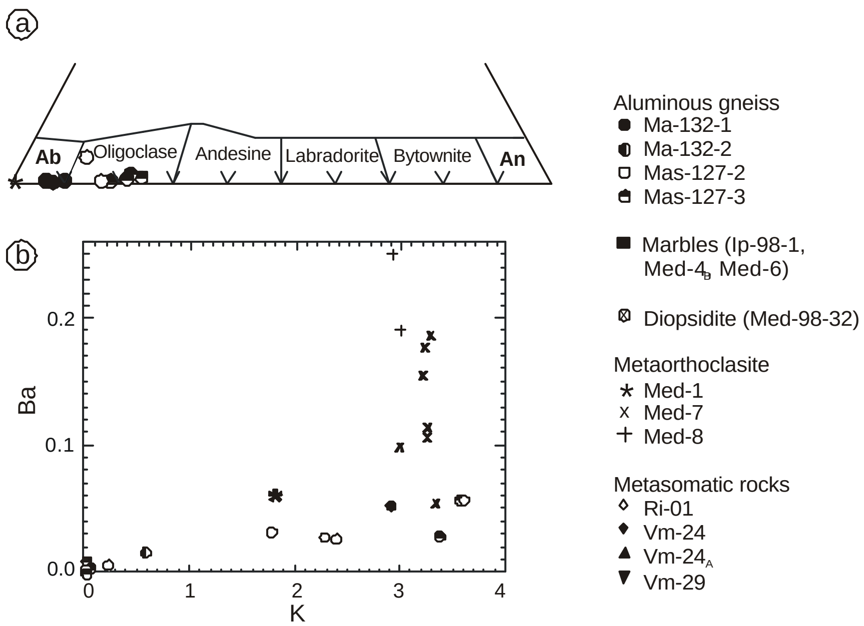

Figure 3: a- Compositional field for plagioclase from aluminous gneiss. b- K x Ba diagram in p.f.u. (atoms per formula unit).

Table 1: Representative analyses of feldspar, cordierite, garnet and spinel (samples Ma-132-1, Mas-127-2, Mas-127-3: aluminous gneiss; Med-1, Med-7, Med-8: metaorthoclasite; Vm-24: garnet epidosite).

MINERAL	feldspar										cordierite	
SAMPLE	Mas-127-2	Mas-127-2	Mas-127-3	Mas-127-3	Ma-132-1	Ma-132-1	Med-1	Med-7	Med-8		Ma-132-1	Ma-132-1
ANALYSIS	71	72	99	100	371	370	145	368	148		376	388
SiO_2	65.18	64.66	63.27	63.92	67.39	65.58	65.94	63.39	63.02		49.11	49.44
TiO_2	0.08	0.02	0.02	0.02	0.04	0.11	0.04	0.05	0.02		0.04	0.01
Al_2O_3	22.31	18.49	23.14	18.42	21.06	18.92	18.97	18.94	19.36		33.75	34.01
FeO	0.02	0.05	-	-	0.05	-	0.38	0.03	0.06		4.11	5.28
MnO	0.00	0.01	-	-	-	0.01	-	-	0.02		-	-
MgO	0.02	0.00	-	-	-	0.00	0.02	-	-		11.60	10.87
BaO	0.04	0.79	0.10	0.77	-	0.72	0.83	2.53	3.44		n.d.	n.d.
SrO	0.06	-	0.03	-	0.03	0.02	0.12	0.07	0.18		n.d.	n.d.
ZnO	n.d.	n.d.	n.d.	n.d.	n.d.	n.d.	n.d.	n.d.	n.d.		0.24	0.10
CaO	3.41	0.08	4.39	0.01	1.65	0.25	0.11	-	0.02		-	-
Na_2O	9.43	0.83	8.87	1.02	10.88	2.91	5.87	1.42	2.22		-	0.03
K2O	0.13	15.32	0.19	15.01	0.08	12.60	7.84	13.81	12.21		-	-
TOTAL	100.69	100.24	100.01	99.18	101.16	101.13	100.11	100.22	100.54		98.85	99.75
AB	82.70	7.60	77.70	9.40	91.90	25.70	52.90	13.50	21.60	X_{Mg}	0.83	0.78
AN	16.50	0.40	21.20	0.10	7.70	1.20	0.50	0.00	0.10			
OR	0.70	92.10	1.10	90.50	0.40	73.10	46.50	86.50	78.30			

MINERAL	garnet							spinel			
SAMPLE	Ma-132-1	Ma-132-1	Mas-127-2	Mas-127-2	Mas-127-2	Vm-24		Mas-127-2	Mas-127-3	Ma-132-1	Ma-132-1
ANALYSIS	333	387	51	52	55	292		48	69	374	379
SiO_2	38.43	37.95	38.20	38.86	38.02	37.25		0.02	0.01	-	-
TiO_2	0.03	-	-	-	-	0.67		0.02	0.03	0.04	-
Al_2O_3	22.87	21.76	21.98	22.24	21.86	17.15		58.85	58.53	57.63	61.14
Cr_2O_3	-	-	-	-	-	2.80		-	0.03	0.28	0.04
Fe_2O_3	1.58	1.80	1.69	1.55	1.76	6.80		0.05	1.70	2.93	1.33
FeO	27.08	30.75	28.92	26.57	30.06	6.12		19.02	24.94	26.76	19.03
Y_2O_3	-	0.06	0.01	0.02	-	0.04		n.d.	n.d.	n.d.	n.d.
MnO	0.11	0.17	0.51	0.47	0.71	0.58		0.02	0.08	-	-
MgO	11.03	7.89	8.16	10.20	7.29	0.88		6.96	5.91	5.83	10.60
NiO	n.d.	n.d.	n.d.	n.d.	n.d.	n.d.		-	0.03	0.04	-
ZnO	n.d.	n.d.	n.d.	n.d.	n.d.	n.d.		11.18	7.35	5.59	6.58
CaO	0.35	0.38	0.41	0.53	0.56	26.47		-	-	-	-
Na_2O	-	0.01	0.02	0.01	0.03	-		n.d.	n.d.	n.d.	n.d.
K_2O	0.01	0.01	-	-	0.01	-		n.d.	n.d.	n.d.	n.d.
Nb_2O_5	n.d.	n.d.	n.d.	n.d.	n.d.	n.d.		-	-	-	-
P_2O_5	n.d.	n.d.	n.d.	n.d.	n.d.	n.d.		-	-	-	-
TOTAL	101.34	100.59	99.73	100.31	100.11	98.09		96.12	98.59	99.11	98.73
X_{Mg}	0.42	0.31	0.33	0.40	0.29	0.04	X_{Mg}	0.30	0.25	0.25	0.43
ALM	48.51	59.02	64.98	57.86	67.58	14.51	X_{Fe}	0.46	0.59	0.64	0.43
PRP	50.07	39.14	32.68	39.61	29.20	3.73	X_{Zn}	0.24	0.15	0.12	0.13
AND	1.12	1.37	1.18	1.48	1.61	21.76					
GRS	-	-	-	-	-	49.20					

Quartzite

It is only locally observed. Small tabulate orientated crystals of green mica are commonly observed, with green pale pleochroism. Its composition is that of chromian muscovite ("fuchsite") with variable Cr_2O_3 contents (1.5-4.5%, meanly around 4%, Table 2).

Metaorthoclasite

These rocks are formed predominantly by alkaline feldspar, with subordinate clinopyroxene and amphibole. Mesoperthites are common. The name orthoclasite was adopted based exclusively on the mineral association of this rock, with no genetic implication whatsoever. The protholith of this rock is currently under study.

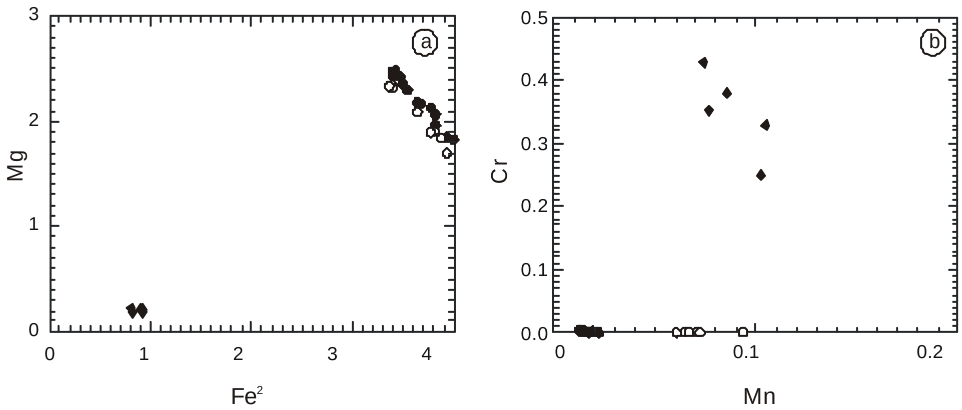

Figure 4: a- Fe^{+2} x Mg diagram for garnet in aluminous gneiss and garnet epidosite. b- Mn x Cr diagram for garnet in aluminous gneiss and garnet epidosite. Values in p.f.u. Symbols as in Figure 3.

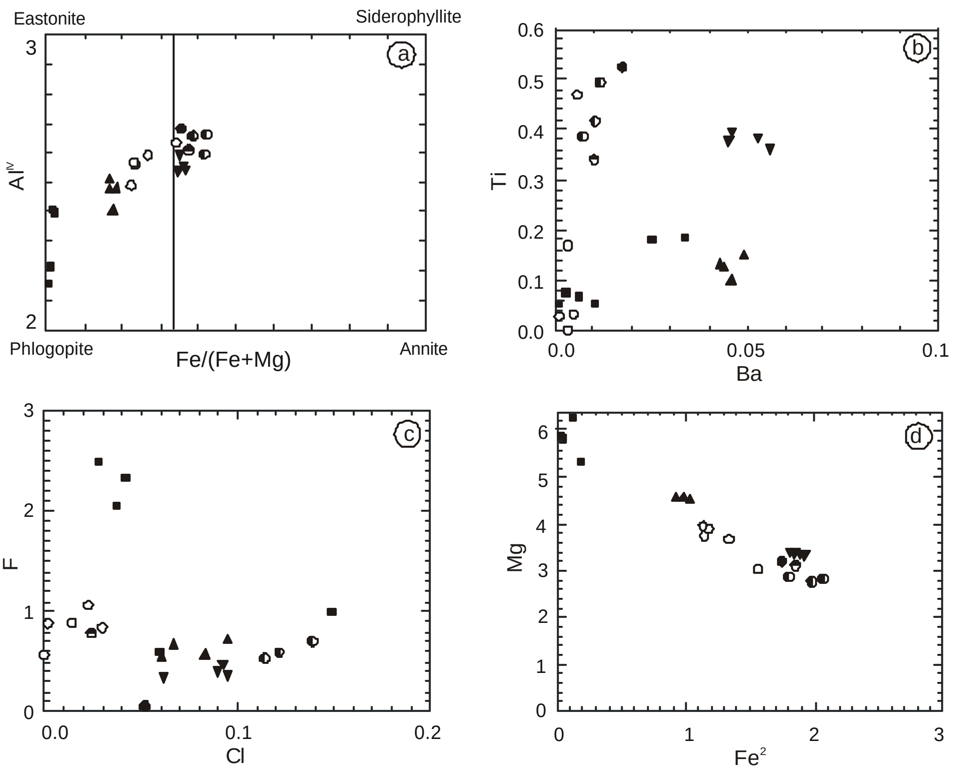

Figure 5: a- Compositional field for biotite. b- Ba x Ti diagram. c- Cl x F diagram. d- Fe^{+2} x Mg diagram. Values in p.f.u. Symbols as in Figure 3.

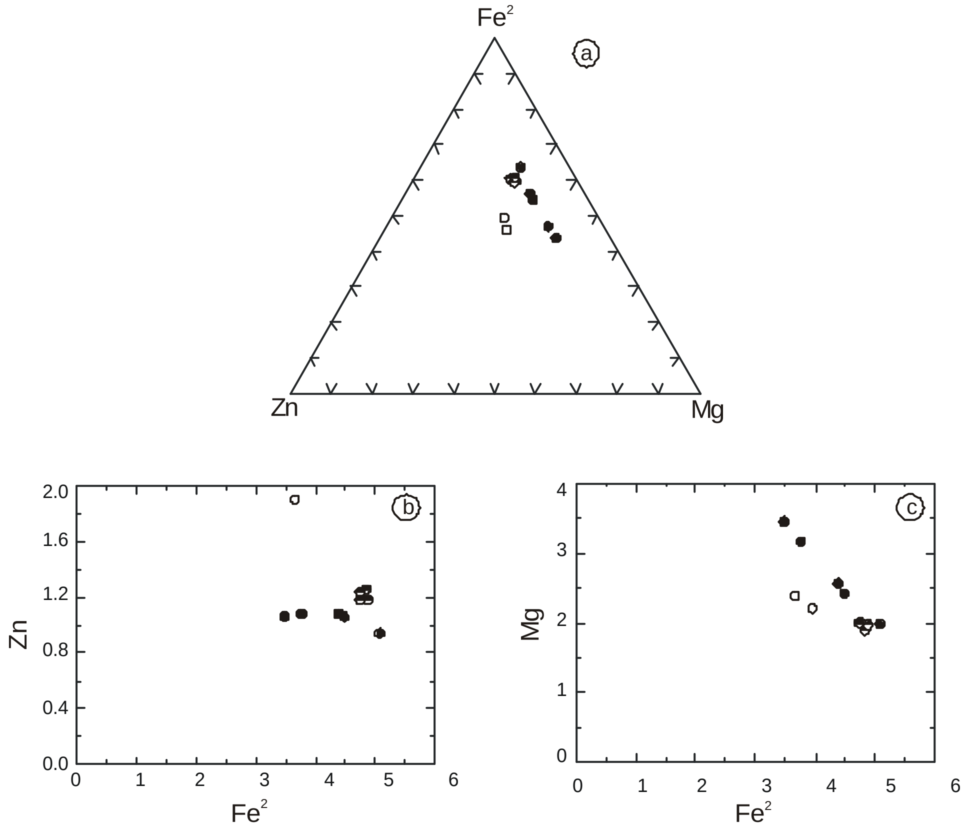

Figure 6: a- Fe^{+2} x Zn x Mg diagram for spinel from aluminous gneiss. b- Fe^{+2} x Zn diagram. c- Fe^{+2} x Mg diagram. Values in p.f.u. Symbols as in Figure 3.

The K-feldspar has high BaO content (Figure 3b), with concentrations ranging from 0.8 to 3.4% (Table 1).

Clinopyroxenes are diopside (sample Med-8), salite (Med-7) and Fe-salite (Med-1) (Figure 7).

Amphibole is actinolite and seems to be originated from clinopyroxene substitution. It shows greenish colour and is also very altered.

Apatite and sphene occur as well developed crystals. Apatite is common and can reach up to 4 mm.

Marble

The serpentine marble is a very characteristic lithology of the metasedimentary sequence. Its particularity are the serpentine "balls" present in the carbonates. Its mineralogy is constituted predominantly by granoblastic carbonates, with olivine "balls" partially or completely substituted by serpentine. Phlogopite, chlorite, talc, apatite and opaques are minor constituents. Olivine is locally preserved. It has a Fo_{96-99} composition, being Mg-richer than the olivines of the ultramafic rocks. Its low NiO content (0.04%) indicates a different genesis with regard to the olivine of the ultramafic sequence. Serpentine occurs in the "balls" and along threads or bands.

Based on textural features, antigorite seems to prevail among serpentines. Chrysotile, that is more fibrous, also occurs, interlocked with and involving antigorite. In some samples, there are disseminated interstitial carbonates. FeO, MgO and Al_2O_3 contents in serpentines present small variations. Phlogopite seems to be late and is deformed. In the marble, phlogopite practically does not have Cr_2O_3, and presents MgO, TiO_2, BaO and F variations. Its F content is higher than in other petrographic types (Figure 5c).

Brownish balls of fibrous aggregates also occur in the marble and seems to have been phlogopite that altered to chlorite. Chlorite has anomalous blue birefringence, with penninite composition. Apatite is colourless and occurs as

Table 2: Representative analyses of mica, clinopyroxene, olivine and amphibole (samples Ma-132-1, Ma-132-2, Mas-127-2, Mas-127-2, Mas-127-3: aluminous gneiss; V-98: quartzite; Med-1, Med-7, Med-8: metaorthoclasite; Ip-98-1, Med-4_B, Med-6: marble; Med-98-32: diopsidite; Ri-01, Vm-24, Vm-24_A, Vm-29: metasomatic rocks).

MINERAL	mica												
SAMPLE	Mas-127-2	Mas-127-2	Mas-127-3	Ma-132-1	Ma-132-2	Vm-24_A	Vm-29	Ip-98-1	Med-4_B	Med-6	Ri-01	V-98	Vm-24
ANALYSIS	42	45	95	382	38	1	5	49	112	122	8	4	295
SiO_2	38.22	37.05	36.01	35.97	36.20	37.91	36.68	41.55	39.94	39.14	45.88	45.14	45.36
TiO_2	0.28	4.32	3.05	4.71	3.76	1.19	3.24	0.63	1.75	0.62	-	0.24	-
Al_2O_3	20.33	18.75	17.40	17.03	17.74	16.40	15.72	14.06	16.00	14.46	40.86	35.45	37.17
Cr_2O_3	-	-	0.01	0.01	0.05	0.18	0.08	0.04	0.03	0.02	-	4.52	-
FeO	9.91	12.91	14.79	14.20	16.79	7.60	14.58	0.36	1.44	1.21	0.12	0.86	0.16
MnO	-	0.02	0.02	-	0.01	0.04	0.08	0.02	-	0.01	-	0.16	0.02
MgO	18.40	14.02	13.94	14.58	12.88	21.16	15.30	28.11	25.28	30.13	0.41	0.41	-
BaO	0.01	0.11	0.16	0.31	0.17	0.76	0.97	0.11	0.47	0.11	0.09	0.03	-
CaO	-	-	-	-	-	0.02	0.02	0.03	0.14	0.08	0.27	-	0.13
Na_2O	0.08	0.07	0.06	0.09	0.16	0.17	0.12	0.25	0.55	0.32	0.18	0.32	0.09
K_2O	9.63	9.85	9.90	9.18	9.80	9.17	9.36	10.28	9.23	6.88	10.49	10.08	10.78
F	1.07	0.57	0.78	0.06	0.54	0.67	0.47	2.04	0.59	0.97	-	0.63	-
Cl	0.02	-	0.02	0.05	0.11	0.07	0.09	0.04	0.06	0.15	0.01	0.01	0.02
H2O	3.71	3.87	3.63	4.02	3.78	3.78	3.78	3.33	3.97	3.74	4.68	4.25	4.46
TOTAL	101.66	101.54	99.77	100.21	101.98	99.11	100.49	100.83	99.44	97.82	102.98	102.09	98.18
X_{Mg}	0.77	0.66	0.63	0.65	0.58	0.83	0.65	0.99	0.97	0.98	0.86	0.46	0.00

MINERAL	clinopyroxene						olivine		amphibole	
SAMPLE	Med-1	Med-7	Med-8	Med-98-32	Ri-01	Vm-24_A	Ip-98-1	Med-4_B	Med-7	Ri-01
ANALYSIS	137	395	138	4	10	20	59	128	393	11
SiO_2	50.64	53.15	53.12	55.11	52.32	53.17	42.75	41.91	55.86	55.72
TiO_2	0.08	-	0.24	-	0.27	-	-	0.00	-	0.29
Al_2O_3	0.73	0.87	1.95	0.29	3.68	1.02	-	-	0.42	2.21
Cr_2O_3	-	0.04	0.03	-	-	0.10	-	-	0.02	0.08
FeO	18.89	6.89	4.02	0.20	3.40	5.19	1.48	4.00	8.12	4.44
MnO	0.27	0.63	0.64	0.07	0.16	0.17	0.29	0.34	0.47	0.09
NiO	0.01	-	0.03	-	-	-	0.05	0.03	n.d.	n.d.
MgO	6.39	13.86	14.15	19.04	15.70	16.21	57.77	52.68	19.09	20.62
CaO	19.84	24.07	24.24	25.33	24.90	23.29	0.03	0.03	12.83	13.79
Na_2O	2.09	0.42	0.63	0.08	0.11	0.30	-	-	0.12	0.16
BaO	n.d.	n.d.	n.d.	n.d.	n.d.	n.d.	n.d.	n.d.	-	-
K_2O	n.d.	n.d.	n.d.	n.d.	n.d.	n.d.	n.d.	n.d.	0.03	0.02
F	n.d.	n.d.	n.d.	n.d.	n.d.	n.d.	n.d.	n.d.	-	-
Cl	n.d.	n.d.	n.d.	n.d.	n.d.	n.d.	n.d.	n.d.	-	-
TOTAL	98.93	99.92	99.05	100.13	100.53	99.44	102.4	98.98	96.94	97.34
WO	45.40	48.89	51.00	48.68	50.27	46.56				
EN	20.40	39.17	41.40	50.91	44.11	45.09				
FS	34.20	11.94	7.60	0.41	5.62	8.36				

relatively well developed crystals, up to 3 cm (it is usually millimetric). Opaques, mainly magnetite, occur as dispersed subidioblastic crystals. They may outline the chlorite balls.

The carbonates can occur with a serpentine aureole, suggesting a reaction rim. They seem to assimilate the serpentine, substituting it. Sometimes they have indented contacts. Carbonates are interstitial to or cut across serpentine, indicating a carbonatation process after serpentinization.

Diopsidite

These rocks are characterized by well developed aggregates of diopside (Figure 7). The crystals are altered and very fractured. They present irregular, rounded and prismatic shapes, and may exhibit polygonal texture. Diopside grain size is variable ranging from finely recrystallized portions up to 7 mm crystals. Fine phyllosilicates are in the diopside grains contacts. Discontinuous serpentine veins, and chlorite and carbonate veins, cut randomly the clinopyroxenite.

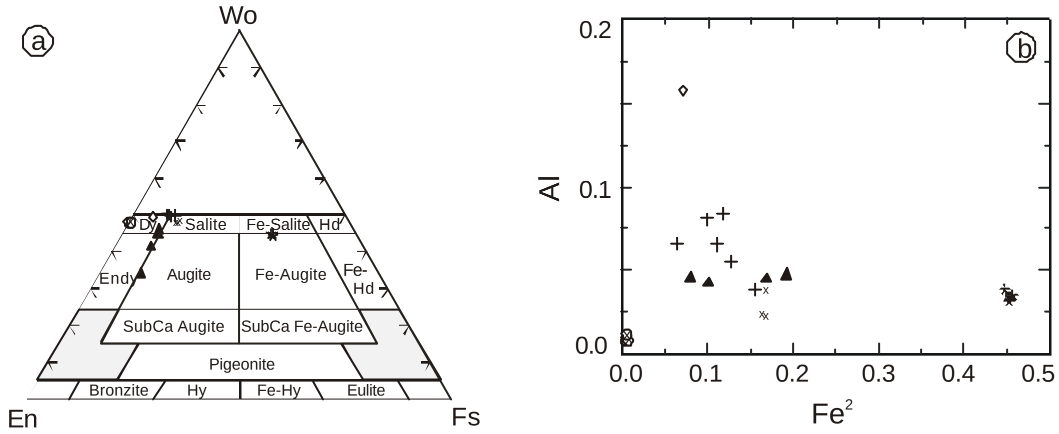

Figure 7: a- Compositional field for clinopyroxene. b- Fe^{+2} x Al diagram. Values in p.f.u. Symbols as in Figure 3.

Rocks with phlogopite and/or clinozoisite

The formation of phlogopite and/or biotite seems to be linked to a late metasomatic process that affected all rocks, both metasedimentary and ultramafic, with varying intensity, on behalf of the preferential fluid percolation paths. The effect of this process upon the metasedimentary rocks is noticed by frequent phlogopite and/or biotite development, concentrated in bands and veins, or randomly distributed in the rock. Phlogopite and biotite are Ba-rich. The metasomatic process is also observed in the ultramafic sequence, where the rocks are cut or involved by phlogopite.

Hydrothermalized clinopyroxenite

These rocks are composed predominantly by clinozoisite and phlogopite or biotite, with clinopyroxene remmants indicating hydrothermalized diopsidites. They present a banded aspect. Clinozoisite has brownish colour and occurs as prismatic crystals that seem to replace clinopyroxene; a crystal with clinopyroxene core and clinozoisite rims has been observed. Some clinozoisite crystals are zoned with epidote cores. Phlogopite (sample Vm-24_A) and biotite (Vm-29) occur as tabulate, isolated or aggregated crystals, with random disposition. It is a Ba-rich variety (Figure 5b) and may show brown or brownish green colours, due to chloritization. Clinopyroxene is mainly diopside (samples Ri-01 and Vm-24_A) and endiopside and augite (Vm-24_A) - Figure 7a. It occurs as irregular, dirty and altered crystals, and may be impregnated by opaques. Amphibole is actinolite and seems to substitute clinopyroxene. Serpentine occurs interstitially. Carbonates occur associated with clinozoisite. Apatite may be common, as round or subidioblastic crystals. Sphene appears as small round crystals. Plagioclase, when present, is completely sericitized and occurs in the clinozoisite- and sphene-rich bands. Carbonate veins are also observed.

Garnet epidosite

Epidote/clinozoisite of brownish colour appears as prismatic crystals or in aggregates. It presents localized yellowish, heterogeneous pleochroism. Clinozoisite is seemingly replaced by epidote, as shown by its anomalous blue birefringence changing to yellow-blue birefringence. Fe and Al contents are variable (Table 3). Garnet shows irregular shapes, with fragments of larger crystals with yellowish colours, intimately associated with epidote. It is Ca-rich with X_{Ca} = 0.8. Cr_2O_3 content is high (2-3% - Figure 4b), and Ti and Fe^{+3} also accur. Completely sericitized plagioclase occurs interstitially to epidote. Opaques appear as xenoblastic crystals, may be well developed or not, and are relatively common. Sphene of brown colour occurs as minuscule punctuations all over the whole rock. Apatite is also present, and has higher SrO content than in other samples (Table 3). Locally muscovite is observed (Table 2). Carbonates occur impregnating the assemblage, associated with alteration.

Table 3: Representative analyses of apatite, serpentine and epidote (samples Ip-98-1, $Med\text{-}4_B$, Med-6: marble; Med-7: metaorthoclasite; Ri-01, Vm-24, $Vm\text{-}24_A$, Vm-29: metasomatic rocks).

MINERAL	apatite					serpentine					epidote		
SAMPLE	Ip-98-1	Med-7	Vm-24	$Vm\text{-}24_A$	Vm-29	Ip-98-1	$Med\text{-}4_B$	$Med\text{-}4_B$	Med-6	Ri-01	Vm-24	Vm-24	Vm-24
ANALYSIS	55	399	308	24	28	51	111	114	121	14	325	326	328
SiO_2	0.06	0.48	0.06	0.34	0.45	39.66	39.49	42.07	41.31	39.21	37.46	39.09	38.27
TiO_2	n.d.	n.d.	n.d.	n.d.	n.d.	-	0.02	0.01	0.04	-	0.01	0.03	-
Al_2O_3	n.d.	n.d.	n.d.	n.d.	n.d.	0.09	0.28	0.12	0.83	35.65	26.62	33.28	29.90
Cr_2O_3	n.d.	n.d.	n.d.	n.d.	n.d.	-	-	0.01	-	-	-	-	-
FeO	-	-	0.02	0.09	0.22	0.45	3.83	1.54	1.06	0.46	8.18	1.94	5.40
MnO	0.01	0.02	0.02	-	0.02	0.20	0.07	0.03	0.06	0.06	0.00	0.02	0.02
MgO	-	0.01	0.01	0.05	-	41.34	40.18	41.55	40.53	0.29	0.01	0.02	0.01
CaO	55.18	53.40	54.73	53.17	54.39	0.02	0.04	0.03	0.05	24.34	23.42	24.04	24.01
BaO	0.05	0.11	0.12	0.00	0.00	0.04	0.01	0.12	0.08	0.07	-	-	-
SrO	0.01	0.07	-	1.15	0.44	n.d.	n.d.	n.d.	n.d.	0.27	-	-	-
Na_2O	0.04	0.08	-	0.07	0.04	-	0.01	0.01	0.02	-	-	-	-
K_2O	n.d.	n.d.	n.d.	n.d.	n.d.	0.01	0.01	-	0.01	-	-	0.01	-
P_2O_5	41.21	40.47	41.75	41.72	42.13	n.d.	n.d.	n.d.	n.d.	n.d.	n.d.	n.d.	n.d.
La_2O_3	-	0.38	0.01	0.18	0.09	n.d.	n.d.	n.d.	n.d.	-	-	-	0.09
Ce_2O_3	-	0.50	-	0.43	0.73	n.d.	n.d.	n.d.	n.d.	-	0.02	-	0.06
Y_2O_3	n.d.	n.d.	n.d.	n.d.	n.d.	n.d.	n.d.	n.d.	n.d.	0.04	0.01	-	0.02
F	4.07	2.84	2.92	3.57	3.67	0.03	0.02	0.04	0.07	n.d.	n.d.	n.d.	n.d.
Cl	0.32	0.69	0.33	0.53	0.25	0.07	0.42	0.04	0.08	n.d.	n.d.	n.d.	n.d.
TOTAL	100.95	99.03	99.97	101.31	102.42	81.90	84.26	85.55	84.09	100.38	95.72	98.43	97.79

METAMORPHISM

Metamorphic aspects were detailed for metasedimentary rock types, which are more favourable for recovering the record of the metamorphic processes which took place in the area.

The marbles present a very simple mineralogy, essentially represented by olivine and calcite, with olivine replaced by serpentine.

As observed in Figure 8, the forsterite-calcite±dolomite association is stable under conditions above reactions 5 and 6. Carbonate from the analysed samples corresponds to calcite, however the presence of dolomite can not be excluded. Diopside and tremolite are not observed, if these phases existed, they were already transformed.

Considering that the metamorphism is essentially anhydrous, developed under high X_{CO_2} conditions, the forsterite-calcite association has probably derived from the reaction Di + 3Dol = 4Cal + 2Fo + $2CO_2$. The variation of the equilibrium conditions as a function of pressure for different values of T - X_{CO_2} are presented in Figure 9, obtained from Berman (1991). In the 4 to 7 kb pressure range, the association is stable for temperatures up to 710-810ºC, respectively.

Olivine serpentinization possibly occured under distinct conditions: as seen in Figure 10, serpentine has its stability limited to a field below approximately 500ºC and of low X_{CO_2} (around 5%). If X_{CO_2} is higher, the Tlc + Mgs or Qtz + Mgs (see, respectively, curves 3 and 5 of Figure

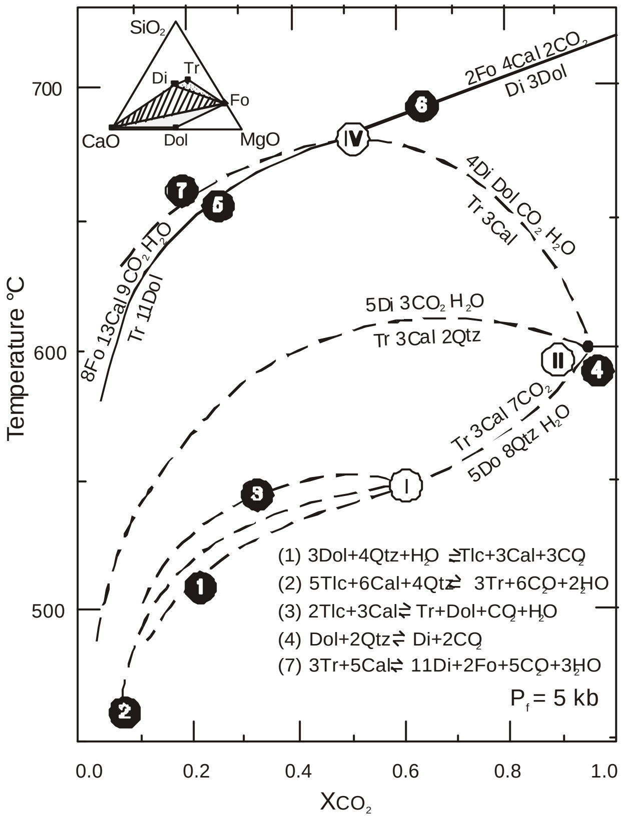

Figure 8: Isobaric T-X_{CO_2} diagram for reactions in siliceous dolomites (Winkler, 1979).

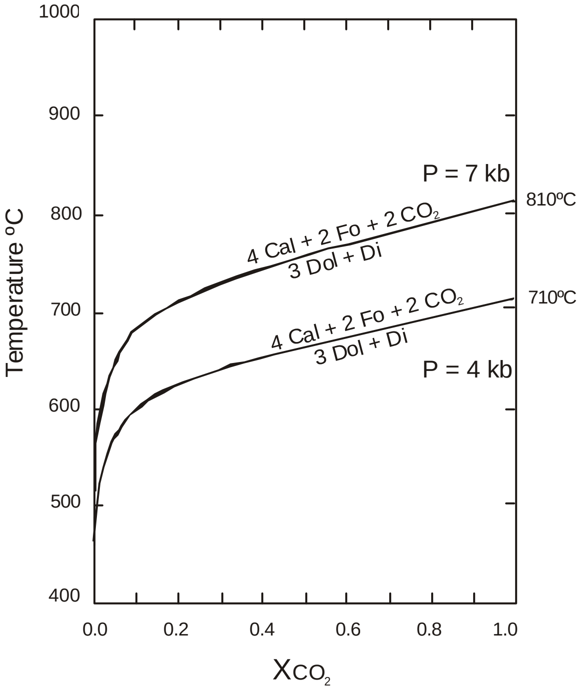

Figure 9: T-X_{CO_2} diagram showing equilibrium conditions of the reaction 4Cal + 2Fo + 2CO_2 = 3Dol + Di for P_T values of 4 kb and 7 kb in a serpentine marble sample (Berman, 1991).

10) associations will appear, which were not observed. The change of olivine to serpentine must be related to a low-temperature hydrothermal/metasomatic process.

The aluminous gneiss presents K-feldspar, quartz, plagioclase, cordierite, garnet, sillimanite and gahnitic hercynite, as a high-grade mineral association.

Phase relations concerning these minerals were analysed by various authors (Hensen, 1971, 1986, 1987; Hensen & Green, 1973; Waters, 1991; Spear, 1993). The phase relations are shown on the diagram of Figure 11, with a Grt-Crd-Sil field in evidence, as well as one for Spl-Qtz-Crd, separated by the reaction Grt+Crd+Sil= Spl+Qtz. It is important to mention, however, that these phase relations are true when spinel contains little or no zinc, whilst the spinel in the analysed samples is fairly rich (6-11%) in this element. Granulite facies rocks often exhibit hercinitic spinels with variable ZnO content, e. g., Adirondacks (Stoddard, 1979); Ardèche (Weber & Barbey, 1986); Central Australia (Clarke *et al*., 1990); Eastern Ghats Belt, India (Dasgupta *et al*., 1995), Mariana - Minas Gerais State, Brazil (Candia, pers. comm.).

The influence of zinc over the spinel stability field has been analysed by Nichols *et al*. (1992). This element increases the spinel stability field to higher pressures and

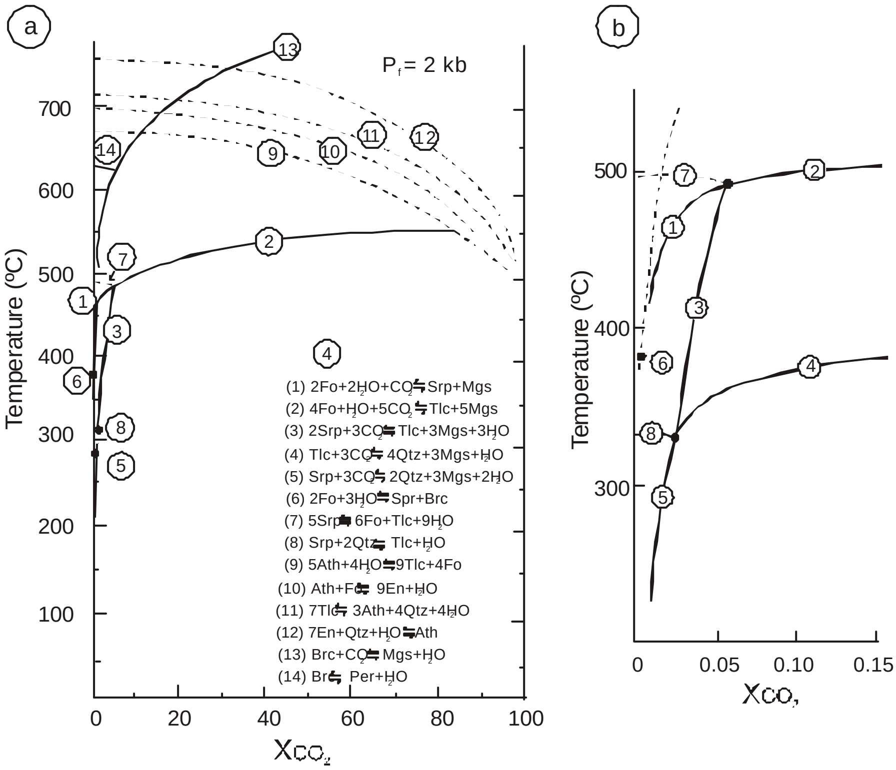

Figure 10: a- Isobaric equilibrium reaction curves in the system MgO-SiO_2-H_2O-CO_2 (Johannes, 1969; simplified). b- Detail of reactions 3 and 5.

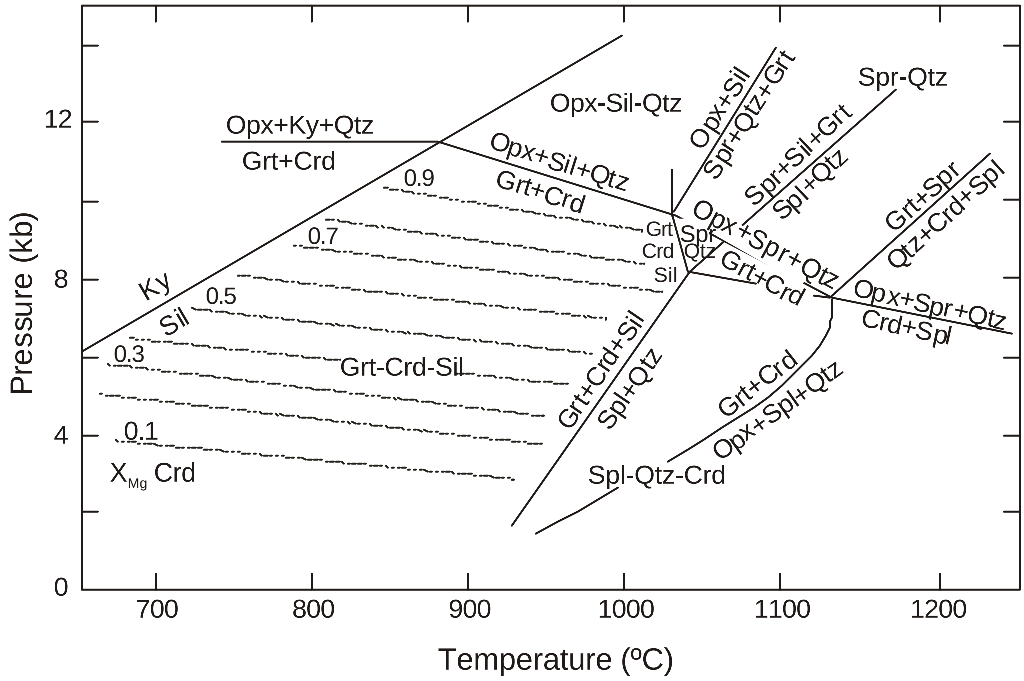

Figure 11: P-T diagram showing Grt-Crd-Sil field at low oxygen fugacity. Isopleths for X_{Mg} in cordierite (after Hensen & Green, 1973).

lower temperatures. Eventually the presence of zinc stabilizes spinel in the Crd-Grt-Sil association.

The stability field for this association is fairly large, attaining 900-1,000ºC, depending on the pressure. To better delimitate the P-T field, Spl-Crd-Sil-Qtz thermobarometry, which takes into account Zn as a component, was applied (Nichols *et al*., 1992), thus obtaining 765ºC and pressures between 8.7 kb (in water-saturated systems - FASHZn and MASHZn) and 6.2 kb (in dry systems - FASZn and MASZn) for spinels included in garnet (Figure 12a). The 8.5 kb pressure is obtained also through the Crd-Spl-Qtz barometer (Perchuk, 1991).

Nichols *et al*. (1992) also developed a Grt-Crd-Sil-Qtz thermobarometer which yielded P-T conditions of 680ºC and 6.1-4.6 kb (for garnet cores and more magnesian cordierite) and 530ºC and 4.5 kb (for garnet rims and more iron-rich cordierite), which are lower than those obtained through the 2.02 TWQ version (Berman, 1991), respectively of 698ºC and 7.3 kb and 665ºC and 6.4 kb for the same phases (Figure 12b,c). Results are synthesized in Table 4 and Figure 13.

These results indicate high-grade metamorphic conditions, with pressures in the 7-8 kb range and temperatures around 800ºC. Some results might reflect Fe-Mg reequilibria among the phases under decreasing P-T conditions. These results suggest a high amphibolite to granulite facies metamorphic environment.

An interesting aspect to be further detailed refers to the behaviour of spinel, which exhibits X_{Mg} both higher and lower than garnet (Figure 14). A similar behaviour is mentioned by Nichols *et al*. (1992), with spinel X_{Mg} either lower, equal to or higher than that of garnet, with the inflection point representing the appearance of cordierite in the association.

The above mentioned P-T conditions already embrace the anatexis field for rocks of suitable compositions, depending on fluid availability. Anatectic pockets and pegmatoid veins can be locally observed in the outcrops.

METASOMATIC PROCESSES

The country-rocks, as well as the ultramafic sequence, are strongly affected by metasomatic processes. The common and expressive occurrence of phlogopite or biotite sometimes together with amphibole, indicates a strong secondary transformation of these rocks.

Phlogopite is Ba-rich, element that may be brought by metasomatic fluids. Serpentinization of the olivine "balls" and the phlogopitization of the marbles could be due to

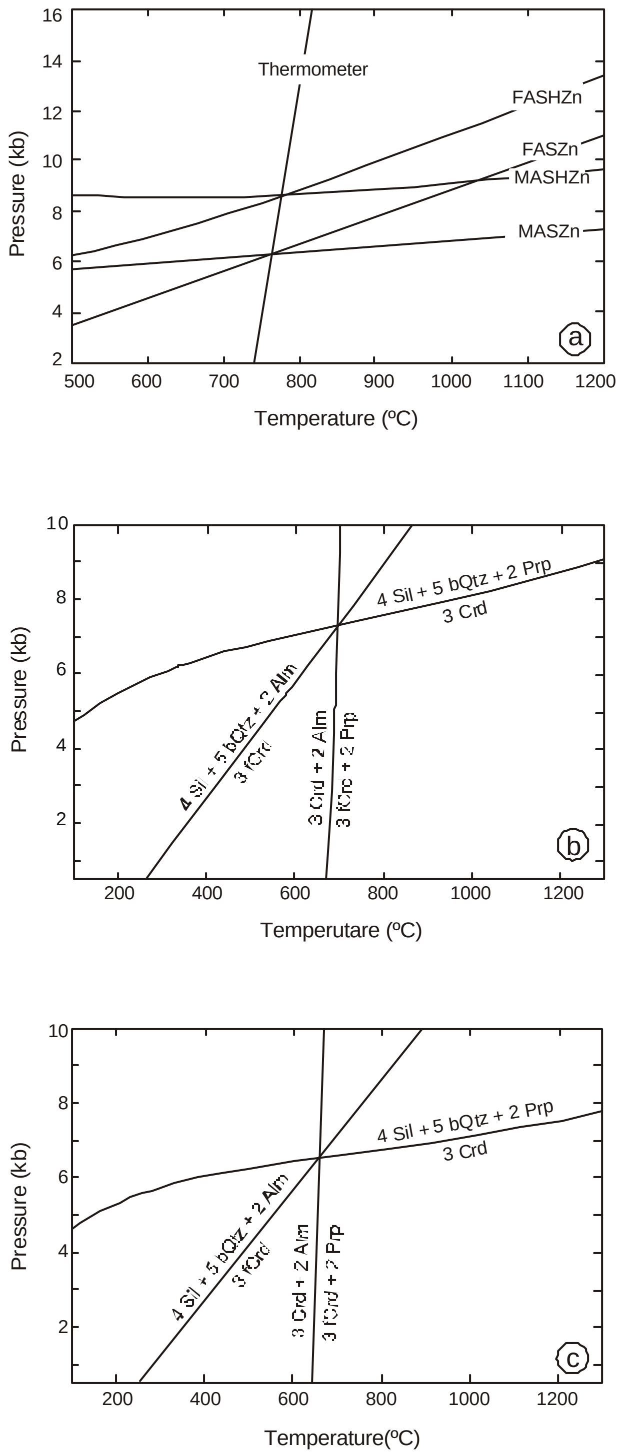

Figura 12: a- P-T diagram for aluminous gneiss showing the Spl-Crd-Sil-Qtz thermobarometer of Nichols *et al*. (1992). b- P-T diagram for aluminous gneiss showing thermobarometric results by TWQ (Berman, 1991) for garnet core. c- As above, for garnet rim.

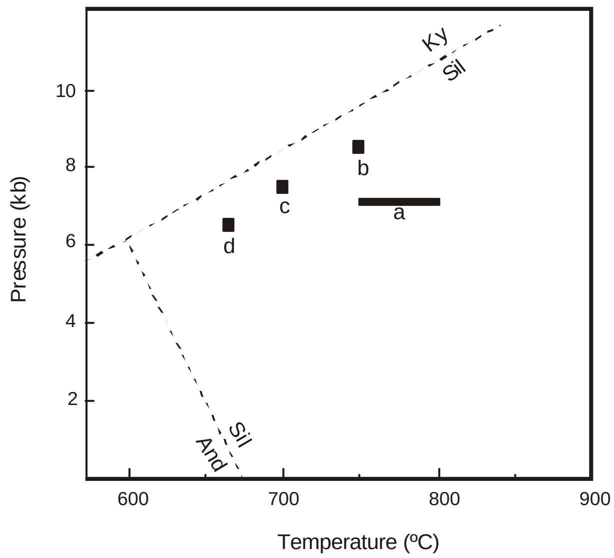

Figure 13: P-T diagram for marble (a) and aluminous gneiss (b, c, d). (b) was obtained by Spl-Crd-Sil-Qtz (Nichols *et al*., 1992) and Crd-Spl-Qtz (Perchuk, 1991) associations. (c) and (d) were obtained by TWQ (Berman, 1991) for garnet core and rim.

this low-temperature event. Phlogopitization is later than the serpentinization, since phlogopite crystals cut serpentinized minerals.

Besides phlogopite, the presence of apatite (F-rich) and sphene, high-Ba feldspar-bearing rocks and rocks with epidote/clinozoisite and/or garnet are complementary evidences for a metasomatic event.

Kempton (1987) claims that mica introduction into a system increases the amount of some elements, such as Ti, Al, Rb, Sr and Ba. Following this, Ba found in some K-feldspar and Sr in apatite could have been originated from the phlogopitization process or derived from late hydrothermal infiltration.

CONCLUSIONS

The chromite bearing mafic-ultramafic rocks of the Jacurici Valley are deformed, metamorphosed and transformed by metasomatic processes, making it difficult to interpret their evolutive record.

In spite of the metasedimentary country-rocks having also been affected by the processes mentioned above, it is possible to recover their metamorphic record. These rocks were studied to aid in the interpretation of the metamorphic/evo-

Table 4: Thermobarometric data for aluminous gneiss.

	TWQ GRT-CRD-SIL	SPL-CRD-SIL-QTZ (Nichols *et al.*, 1992)	GRT-CRD-SIL-QTZ (Nichols *et al.*, 1992)	CRD-SPL-QTZ (Perchuck, 1991)
Grt core	698ºC e 7.3 kb	770ºC and 8.7 kb (FMASHZn)	680ºC and 6.1 kb	8.5 kb
		760ºC and 6.2 kb (FMASHZn)	4.6 kb	
Grt rim	665ºC e 6.4 kb		530ºC and 4.5 kb	

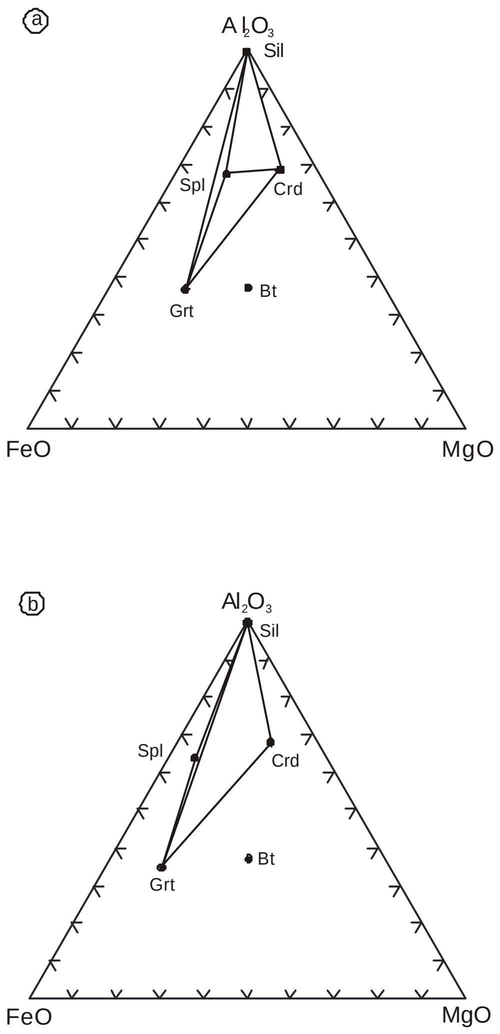

Figure 14: AFM compatibility relations for aluminous gneiss.
a- For garnet core and Mg-richer spinel ($X_{Mg}^{spinel} > X_{Mg}^{garnet}$).
b- For garnet rim and Mg-poorer spinel ($X_{Mg}^{spinel} < X_{Mg}^{garnet}$).

lutionary history of the area. In the pelitic metasediments the data obtained indicate P-T conditions for the highest metamorphic record around 750-800ºC and 7-8 kb.

The rocks of this sequence were subjected to strong phlogopitization. It is not clear whether there was only one metasomatic event or various metasomatic episodes. Phlogopitization is observed to have happened after serpentinization, and also after the carbonatation episode, but it has not been possible so far to establish the chronological relationship of this last event.

ACKNOWLEDGEMENTS

The authors thank FAPESP for the pos-doctoral fellowship (proc. nº. 98/00681-6) to Del Lama and Research Project financing (proc. nº. 97/00640-5); and Prof. Dr. Antenor Zanardo for the valuable petrographic discussions.

REFERENCES

BARBOSA, J.S.F.; DOMINGUEZ, J.M.L. (1996) **Geologia da Bahia**: texto explicativo para o mapa geológico ao milionésimo. Salvador, SGM. 400 p.

BARBOSA, O. (1964) **Geologia de parte da região do médio São Francisco, Nordeste do Brasil**. Petropólis, Prospec. 69 p.

BARBOSA, O. (1970) Geologia de parte da região do médio São Francisco, Nordeste do Brasil. **Boletim DNPM/DFPM**, n. 140, p. 1-98.

BARBOSA DE DEUS, P.; VIANA, J.S. (1982) Jacurici valley chromite district. In: INTERNATIONAL. SYMPOSIUM ON ARCHEAN AND EARLY PROTEROZOIC GEOLOGIC EVOLUTION AND METALLOGENESIS, Salvador, 1982. **Abstracts and Excursions**. Salvador, SBG/CPM. p. 97-107.

BERMAN, R.G. (1991) Thermobarometry using multi-equilibrium calculations: a new technique, with petrological applications. **Canadian Mineralogist**, v. 29, p. 833-855.

CLARKE, G.L.; COLLINS, W.J.; VERNON, R.H. (1990) Sucessive overprinting granulite facies metamorphic events in the Anmatjira Range, central Australia. **Journal of Metamorphic Geology**, v. 8, n. 1, p. 65-88.

DASGUPTA, S.; SENGUPTA, P.; EHL, J.; RAITH, M.; BARDHAN, S. (1995) Reaction textures in a suite of spinel granulites from the Eastern Ghats Belt, India: evidence for polymetamorphism, a partial petrogenetic grid in the system KFMASH and the roles of ZnO and Fe2O3. **Journal of Petrology,** v. 36, n. 2, p. 435-461.

FIGUEIREDO, M.C.H. (1981) Geoquímica das rochas metamórficas de alto grau no nordeste da Bahia, Brasil. In: INCA, H.A.V. **Geologia e recursos minerais do Estado da Bahia:** textos básicos. Salvador, SGM/CPM. v. 4, p. 1-71.

HENSEN, B.J. (1971) Theoretical phase relations involving cordierite and garnet in the system MgO-FeO-Al2O3-SiO2. **Contributions to Mineralogy and Petrology**, v. 33, n. 3, p. 191-214.

HENSEN, B.J. (1986) Theoretical phase relations involving cordierite and garnet revisited: the influence of oxygene fugacity on the stability of sapphirine and spinel in the system Mg-Fe-Al-Si-O. **Contributions to Mineralogy and Petrology,** v. 92, n. 3, p. 362-367.

HENSEN, B.J. (1987) P-T grids for silica-undersatured granulites in the systems MAS (n + 4) and FMAS (n + 3) - tools for the derivation of P-T paths of metamorphism. **Journal of Metamorphic Geology**, v. 5, n. 2, p. 255-271.

HENSEN, B.J.; GREEN, D.H. (1973) Experimental study of the stability of cordierite and garnet in pelitic compositions at high pressures and temperatures III. Synthesis of experimental data and geological applications. **Contributions to Mineralogy and Petrology**, v. 38, n. 2, p. 151-166.

JARDIM DE SÁ, E.F. (1984) **Geologia da região do Vale do Jacurici**. Natal, 17p. (Relatório de Consultoria para CPM).

JOHANNES, W. (1969) An experimental investigation of the system MgO-SiO2-H2O-CO2. **American Journal of Science**, v. 267, n. 9, p. 1083-1104.

KEMPTON, P.D. (1987) Mineralogic and geochemical evidence for differing styles of metasomatism in spinel lherzolite xenoliths: enriched mantle source regions of basalts? In: MENZIES, M.A.; HAWKESWORTH, C.J. (eds.) **Mantle metasomatism**. London, Academic Press, p. 45-89. (Academic Press Geology Series).

KRETZ, R. (1983) Symbols for rock-forming minerals. **American Mineralogist,** v. 68, n. 1/2, p. 277-279.

NICHOLS, G.T.; BERRY, R.F.; GREEN, D.H. (1992) Internally consistent gahnitic spinel-cordierite-garnet equilibria in the FMASHZn system: geothermobarometry and applications. **Contributions to Mineralogy and Petrology,** v. 111, n. 3, p. 362-377.

OLIVEIRA, E.P. (1998) The Cu-rich Caraíba and Cr-rich Medrado mafic-ultramafic complexes, Bahia, Brazil: U-Pb and Nd isotope constraints for archaean lithospheric mantle remobilisation in the Paleoproterozoic Salvador-Curaça Orogen. In: CONGRESSO BRASILEIRO DE GEOLOGIA, 40, Belo Horizonte, 1998. **Anais**. Belo Horizonte, SBG. p. 48.

PERCHUK, L.L. (1991) Derivation of a thermodynamically consistent set of geothermometers and geobarometers for metamorphic and magmatic rocks. In: PERCHUK, L.L. (ed.) **Progress in metamorphic and magmatic petrology.** A memorial volume in honor of D. S. Korzhinskiy. Cambridge, University Press. p. 93-112.

SILVA, L.C.; McNAUGHTON, N.J.; MELO, R.C.; FLETCHER, I.R. (1997) U-Pb SHRIMP ages in the Itabuna-Caraíba TTG high-grade complex: the first window beyond the Paleoproterozoic overprinting of the eastern Jequié craton, NE Brazil. In: INTERNATIONAL SYMPOSIUM ON GRANITES AND ASSOCIATED MINERALIZATIONS, 2, Salvador, 1997. **Extended Abstract and Program**. Salvador, SGM. p. 282-283.

SPEAR, F.S. (1993) **Metamorphic phase equilibria and pressure-temperature-time paths**. Washington, Mineralogical Society of America. 799p. (Monograph).

STODDARD, E.F. (1979) Zinc-rich hercynite in high-grade metamorphic rocks: a product of the dehydration of staurolite. **American Mineralogist**, v. 64, n. 7/8, p. 736-741.

WATERS, D.J. (1991) Hercynite-Quartz granulites: phase relations and implications for crustal processes. **European Journal of Mineralalogy**, v. 3, n. 2, p. 367-386.

WEBER, C.; BARBEY, P. (1986) The role of water, mixing process and metamorphic fabric in the genesis of the Beaume migmatites (Ardèche, France). **Contributions to Mineralogy and Petrology**, v. 92, n. 4, p. 481-491.

WINKLER, H.G.F. (1979) **Petrogenesis of metamorphic rocks**. New York, Springer-Verlag, 348p.